Coupled-Cluster Calculations of Neutrinoless Double-β Decay in ^{48}Ca

S. Novario,[1,2] P. Gysbers,[3,4] J. Engel,[5] G. Hagen,[2,1,3] G. R. Jansen,[6,2] T. D. Morris,[2] P. Navrátil,[3] T. Papenbrock,[1,2] and S. Quaglioni[7]

[1]*Department of Physics and Astronomy, University of Tennessee, Knoxville, Tennessee 37996, USA*
[2]*Physics Division, Oak Ridge National Laboratory, Oak Ridge, Tennessee 37831, USA*
[3]*TRIUMF, 4004 Wesbrook Mall, Vancouver, British Columbia V6T 2A3, Canada*
[4]*Department of Physics and Astronomy, University of British Columbia, Vancouver, British Columbia V6T 1Z1, Canada*
[5]*Department of Physics, University of North Carolina, Chapel Hill, North Carolina 27514, USA*
[6]*National Center for Computational Sciences, Oak Ridge National Laboratory, Oak Ridge, Tennessee 37831, USA*
[7]*Lawrence Livermore National Laboratory, P.O. Box 808, L-414, Livermore, California 94551, USA*

(Received 23 August 2020; revised 15 January 2021; accepted 6 April 2021; published 7 May 2021)

We use coupled-cluster theory and nuclear interactions from chiral effective field theory to compute the nuclear matrix element for the neutrinoless double-β decay of ^{48}Ca. Benchmarks with the no-core shell model in several light nuclei inform us about the accuracy of our approach. For ^{48}Ca we find a relatively small matrix element. We also compute the nuclear matrix element for the two-neutrino double-β decay of ^{48}Ca with a quenching factor deduced from two-body currents in recent *ab initio* calculation of the Ikeda sum rule in ^{48}Ca [Gysbers *et al.*, Nat. Phys. **15**, 428 (2019)].

DOI: 10.1103/PhysRevLett.126.182502

Introduction and main result.—Neutrinoless double-β ($0\nu\beta\beta$) decay is a hypothesized electroweak process in which a nucleus undergoes two simultaneous β decays but emits no neutrinos [1]. The observation of this lepton-number violating process would identify the neutrino as a Majorana particle (i.e., as its own antiparticle) [2] and provide insights into both the origin of neutrino mass [3,4] and the matter-antimatter asymmetry in the Universe [5]. Experimentalists are working intently to observe the decay all over the world; current lower limits on the lifetime are about 10^{26} y [6–8], and sensitivity will be improved by 2 orders of magnitude in the coming years.

Essential for planning and interpreting these experiments are nuclear matrix elements (NMEs) that relate the decay lifetime to the Majorana neutrino mass scale and other measures of lepton-number violation. Unfortunately, these matrix elements are not well known and cannot be measured. Computations based on different models and techniques lead to numbers that differ by factors of 3 to 5 (see Ref. [9] for a recent review). Compounding these theoretical challenges is the recent discovery that, within chiral effective field theory (EFT) [10–13], the standard long-range $0\nu\beta\beta$ decay operator must be supplemented by an equally important zero-range (contact) operator of unknown strength [14]. Efforts to compute the strengths of this contact term from quantum chromodynamics (QCD) [15] and attempts to better understand its impact are underway [16].

The task theorists face at present is to provide more accurate computations of $0\nu\beta\beta$ NMEs, including those associated with contact operators, and quantify their uncertainties. In this Letter, we employ the coupled-cluster method to perform first-principle computations of the matrix element that links the $0\nu\beta\beta$ lifetime of ^{48}Ca with the Majorana neutrino mass scale. Among the dozen or so candidate nuclei for $0\nu\beta\beta$ decay experiments [17], ^{48}Ca stands out for its fairly simple structure, making it amenable for an accurate description based on chiral EFT and state-of-the-art many-body methods [18]. By varying the details of our calculations, we will estimate the uncertainty of our prediction. To gauge the quality of our approach we also compute the two-neutrino double-β decay of ^{48}Ca and compare with data. Our results will directly inform $0\nu\beta\beta$ decay experiments that use ^{48}Ca [19] and serve as an important stepping stone towards the accurate prediction of NMEs in ^{76}Ge, ^{130}Te, and ^{136}Xe, which are candidate isotopes of the next-generation $0\nu\beta\beta$ decay experiments. Calculations in those nuclei presumably require larger model spaces, inclusion of triaxial deformation, and symmetry projection.

Figure 1 shows several recent results for the NME governing the $0\nu\beta\beta$ decay $^{48}\text{Ca} \to {}^{48}\text{Ti}$ and compares them with those of this work. The coupled cluster results obtained here, with both the CCSD and CCSDT-1 approximations (explained below), display uncertainties from details of the computational approach. They are compared to the very recent *ab initio* results from the in-medium similarity group renormalization method with the generator coordinator method (IMSRG + GCM) [20], a realistic shell-model (RSM) [21], the quasiparticle random phase approximation (QRPA) [22], the interacting boson model (IBM) [23], various energy-density functionals (EDF)

 © 2021 American Physical Society

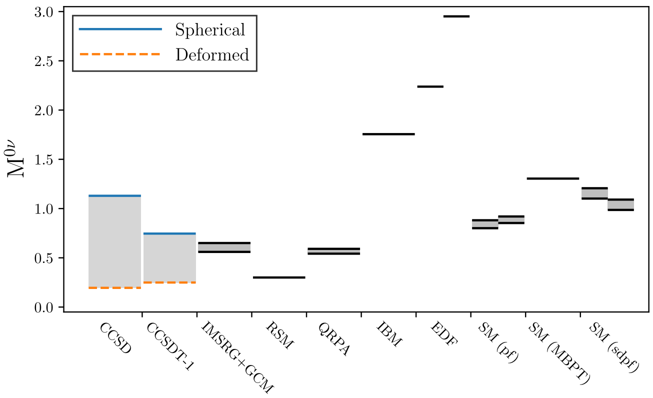

FIG. 1. Comparison of the NME for the $0\nu\beta\beta$ decay of ^{48}Ca, calculated within various approaches (see text for details). The coupled-cluster results use both the CCSD and CCSDT-1 approximations with both the spherical and deformed reference states. For IMSRG + GCM, the double bars show the effects of uncertainty in model-space size; otherwise they show those of uncertainty in short-range correlation functions.

[24,25], and several more phenomenological shell model (SM) calculations. The latter either limit themselves to the pf shell [26,27], include perturbative corrections from outside of the pf shell [28], or are set in the $sdpf$ shell-model space [29]. We see that the *ab initio* results of this work and of Ref. [20] are consistent with each other and with the most recent work [30]. Our result in the CCSDT-1 approximation is $0.25 \leq M^{0\nu} \leq 0.75$.

Method.—We employ the intrinsic Hamiltonian

$$H = \sum_{i<j}\left(\frac{(\vec{p}_i - \vec{p}_j)^2}{2mA} + V_{NN}^{(i,j)}\right) + \sum_{i<j<k} V_{NNN}^{(i,j,k)}. \quad (1)$$

Here m is the nucleon mass, $\vec{p}$ is the momentum operator, A is the mass number of the nucleus, and $V_{NN}^{(i,j)}$ and $V_{NNN}^{(i,j,k)}$ are the nucleon-nucleon (NN) and three-nucleon (NNN) potentials, respectively. We employ the chiral potential 1.8/2.0 (EM) of Ref. [31]. Three-nucleon force contributions are limited to those from matrix elements in the oscillator basis with $N_1 + N_2 + N_3 \leq 16$, where $N_i = 2n_i + l_i$ are single-particle energies. The oscillator basis has a frequency $\hbar\Omega = 16$ MeV and we find that working within a model space with $N_i = 10$ is sufficient to produce converged results.

Following Refs. [32,33], we transform the Hamiltonian from the spherical oscillator basis to a natural-orbital basis by diagonalizing the one-body density matrix. We denote the resulting reference state, i.e., the product state constructed from the A single-particle states with largest occupation numbers, by $|\Phi_0\rangle$ and the Hamiltonian that is normal-ordered with respect to this nontrivial vacuum by H_N. We retain NNN forces at the normal-ordered two-body level [34,35].

Coupled-cluster theory [36–42] is based on the similarity-transformed Hamiltonian, $\bar{H}_N = e^{-\hat{T}} H_N e^{\hat{T}}$. The cluster operator $\hat{T}$ is a sum of particle-hole (ph) excitations from the reference $|\Phi_0\rangle$ and commonly truncated at the two-particle two-hole ($2p$-$2h$) or $3p$-$3h$ level. The amplitudes in $\hat{T}$ are chosen so that the reference state $|\Phi_0\rangle$ becomes the right ground state of $\bar{H}_N$. Because $\bar{H}_N$ is non-Hermitian, the left ground state is $\langle\Phi_0|(1+\hat{\Lambda})$, where $\hat{\Lambda}$ is a deexcitation operator with respect to the reference [41,42]. In this Letter, we work at the leading-order approximation to coupled cluster with singles-doubles-and-triples excitations (CCSDT), known as CCSDT-1 [43,44]. To make the computation feasible, we truncate the $3p-3h$ amplitudes by imposing a cut on the product of occupation probabilities n_a for three particles above the Fermi surface, $n_a n_b n_c \geq \mathcal{E}_3$, and for three holes below the Fermi surface, $(1-n_i)(1-n_j)(1-n_k) \geq \mathcal{E}_3$. This truncation favors orbitals near the Fermi surface. The limits are large enough so that all CCSDT-1 results presented below are stable against changes in them.

We are interested in computing $|M^{0\nu}|^2 = \langle\Psi_I|\hat{O}_{0\nu}^\dagger|\Psi_F\rangle\langle\Psi_F|\hat{O}_{0\nu}|\Psi_I\rangle$, where $\hat{O}_{0\nu}$ is the $0\nu\beta\beta$ operator and Ψ_I and Ψ_F denote the ground states of the initial and final nuclei, respectively. Within coupled-cluster theory, we can structure the calculation in two ways. In a first approach, we can use the right and left ground states of ^{48}Ca ($|\Phi_0\rangle$ and $\langle\Phi_0|(1+\hat{\Lambda})$, respectively) to compute

$$|M^{0\nu}|^2 = \langle\Phi_0|(1+\hat{\Lambda})\overline{O^\dagger}_{0\nu}\hat{R}|\Phi_0\rangle\langle\Phi_0|\hat{L}\overline{O}_{0\nu}|\Phi_0\rangle. \quad (2)$$

In this case, we use equation-of-motion coupled-cluster (EOM-CC) techniques [41,45–50] to represent the right and left ^{48}Ti ground states (denoted by $\hat{R}|\Phi_0\rangle$ and $\langle\Phi_0|\hat{L}$, respectively) by generalized excited states of ^{48}Ca with two more protons and two less neutrons [51,52]. Here, we also work in the CCSDT-1 approximation. In Eq. (2) $\overline{O}_{0\nu} \equiv e^{-\hat{T}}\hat{O}_{0\nu}e^{\hat{T}}$ is the similarity-transformed $0\nu\beta\beta$ operator.

In an alternative approach, we can decouple the ground state of the final nucleus, i.e., take $|\Phi_0\rangle$ as a reference right ground state for ^{48}Ti [with $\langle\Phi_0|(1+\hat{\Lambda})$ its left ground state], and target the initial nucleus ^{48}Ca with EOM-CC. This procedure leads to the expression

$$|M^{0\nu}|^2 = \langle\Phi_0|\hat{L}\overline{O^\dagger}_{0\nu}|\Phi_0\rangle\langle\Phi_0|(1+\hat{\Lambda})\overline{O}_{0\nu}\hat{R}|\Phi_0\rangle, \quad (3)$$

where the ^{48}Ca right and left ground states ($\hat{R}|\Phi_0\rangle$ and $\langle\Phi_0|\hat{L}$, respectively) are represented by generalized excited states of ^{48}Ti. Because the two approaches are identical only when the cluster operators are not truncated, the difference between them is a measure of the truncation effects. As the ground state of ^{48}Ca is spherical, the first procedure allows us to exploit rotational symmetry. By contrast, starting from ^{48}Ti introduces a deformed (though axially symmetric) reference state, which accurately reflects the nontrivial vacuum properties and captures static correlations that would be many-particle–many-hole excitations in the spherical scheme [53]. It comes at the expense of breaking rotational invariance, which eventually could be restored with symmetry restoration techniques [54–56].

In chiral EFT, the $0\nu\beta\beta$ operator is organized into a systematically improvable expansion similarly to the nuclear forces [57]. The lowest-order contributions to the $0\nu\beta\beta$ operator are a long-range Majorana neutrino potential that can be divided into three components, Gamow-Teller (GT), Fermi (F), and tensor (T), that contain different combinations of spin operators, with $\hat{O}_{0\nu} = \hat{O}_{0\nu}^{GT} + \hat{O}_{0\nu}^{F} + \hat{O}_{0\nu}^{T}$. The corresponding two-body matrix elements, as is conventional, are taken from Ref. [58], which adds form factors to the leading and next-to-leading operators. We use the closure approximation (which is sufficiently accurate [26]), with closure energies $E_{\mathrm{cl}} = 5$ MeV for all benchmarks in light nuclei and 7.72 MeV for the decay ${}^{48}\mathrm{Ca} \to {}^{48}\mathrm{Ti}$.

The NME for the $2\nu\beta\beta$ is similar to the $0\nu\beta\beta$ case except the two-body operator is replaced by a double application of the one-body Gamow-Teller operator, $\boldsymbol{\sigma}\tau^-$ [59], with an explicit summation over the intermediate 1^+ states between them,

$$|M^{2\nu}|^2 = \left| \sum_\mu \frac{\langle 0_F^+ | \boldsymbol{\sigma}\tau^- | 1_\mu^+ \rangle \langle 1_\mu^+ | \boldsymbol{\sigma}\tau^- | 0_I^+ \rangle}{\Delta E_\mu + (E_I - E_F)/2} \right|^2. \quad (4)$$

The denominator consists of the excitation energy of the intermediate states with respect to the initial ground state, $\Delta E_\mu = E_\mu - E_I$, and the energy difference between the initial and final states, $E_I - E_F$ (see Supplemental Material [60] and Refs. [73,74] for more details). The direct computation of the matrix element (4) would require several tens of states in the intermediate nucleus and several hundred Lanczos iterations, making it unfeasible in our large model space.

We note that the Green's function at the center of this matrix element can be computed efficiently using the Lanczos (continued fraction) method starting from a 1^+ pivot state [75–79]. We generate Lanczos coefficients (a_i, b_i and a_i^*, b_i^*) from a nonsymmetric Lanczos algorithm using the 1^+ subspace of $\bar{H}_N$ and rewrite Eq. (4) as a continued fraction [75]. This computation typically requires about 10–20 Lanczos iterations. With the similarity-transformed operator, $\overline{O} = \overline{\boldsymbol{\sigma}\tau^-}$, and the pivot states $\langle \nu_F | = \langle \Phi_0 | L \overline{O}$, $|\nu_I\rangle = \overline{O}|\Phi_0\rangle$, $\langle \nu_I | = \langle \Phi_0 | (1 + \hat{\Lambda}) \overline{O}^\dagger$, and $|\nu_F\rangle = \overline{O}^\dagger R |\Phi_0\rangle$, the NME becomes

$$|M^{2\nu}|^2 = \frac{\langle \nu_F | \nu_I \rangle}{a_0 + \frac{E_I - E_F}{2} - \frac{b_0^2}{a_1 + \cdots}} \frac{\langle \nu_I | \nu_F \rangle}{a_0^* + \frac{E_I - E_F}{2} - \frac{(b_0^*)^2}{a_1^* + \cdots}}. \quad (5)$$

Benchmarks.—To gauge the quality of our coupled-cluster computations we benchmark with the more exact no-core shell model (NCSM) [80–82] by computing $0\nu\beta\beta$ matrix elements in light nuclei. Although the $0\nu\beta\beta$ decay of these isotopes are energetically forbidden or would be swamped by successive single-β decays in an experiment, the benchmarks still have theoretical value. Figure 2 shows the $0\nu\beta\beta$ matrix elements of the GT, F, and T operators for the transitions ${}^{6}\mathrm{He} \to {}^{6}\mathrm{Be}$, ${}^{8}\mathrm{He} \to {}^{8}\mathrm{Be}$, ${}^{10}\mathrm{He} \to {}^{10}\mathrm{Be}$, ${}^{14}\mathrm{C} \to {}^{14}\mathrm{O}$, and ${}^{22}\mathrm{O} \to {}^{22}\mathrm{Ne}$. The coupled-cluster results are shown in pairs, with both the initial and final state as the

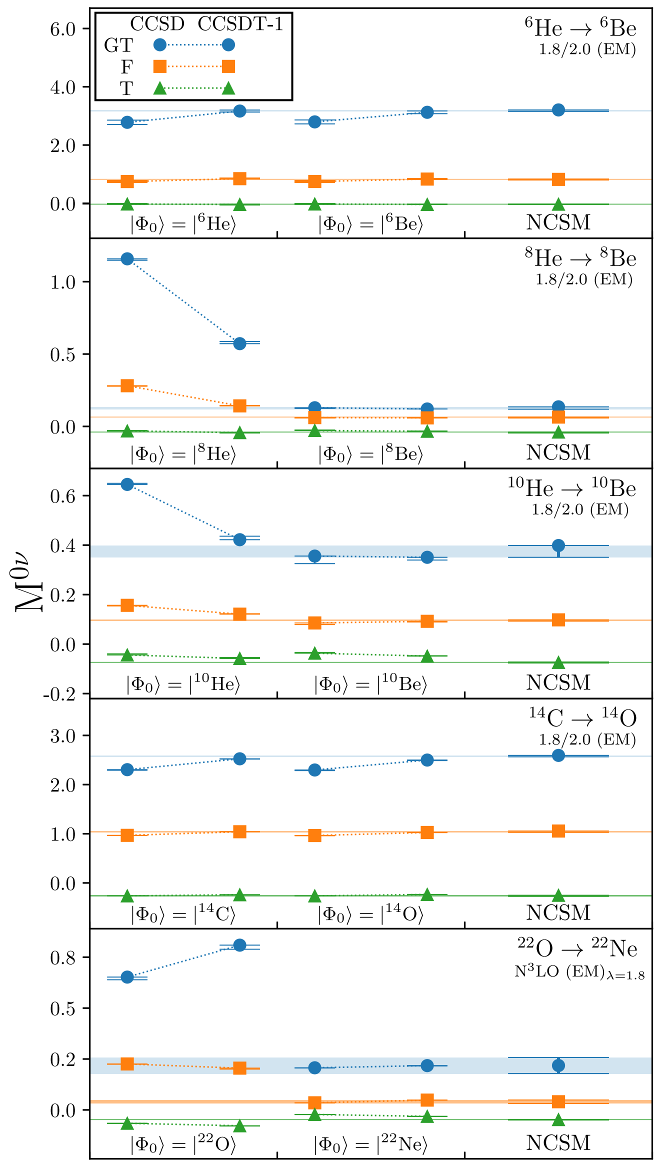

FIG. 2. Comparison of the $0\nu\beta\beta$ NME in several light nuclei computed with the coupled cluster method and the no-core shell model. The first two columns correspond to different choices for the coupled-cluster reference state, and results from the CCSD and CCSDT-1 approximations are shown in each. The error bars indicate the uncertainties coming from variations with model-space size. Each case utilizes the 1.8/2.0 (EM) interaction except for ${}^{22}\mathrm{O} \to {}^{22}\mathrm{Ne}$ which disregards the three-nucleon forces to more rapidly converge the NCSM results.

reference. For each pair, the first (second) point shows the CCSD (CCSDT-1) approximation; these two points are connected by dotted lines. The vertical error bars indicate the change of the matrix element as the model space is increased from $N_{\max} = 8$ to $N_{\max} = 10$. The NCSM results are shown in the third column, and their error bars indicate uncertainties from extrapolation to infinite model spaces. The shaded bands are simply to facilitate comparison.

The NMEs in the mirror-symmetric cases $^{6}\mathrm{He} \to {}^{6}\mathrm{Be}$ and $^{14}\mathrm{C} \to {}^{14}\mathrm{O}$ depend very little (within about 1%) on the choice of the initial or final nucleus as the reference state, a result that is consistent with the weak charge-symmetry breaking of the chiral interaction. For the $A = 14$ transition between doubly closed-shell nuclei, coupled-cluster theory and NCSM results agree within about 3%. The small contributions of triples correlations ($< 10\%$) suggest that these results are accurate. The results are of similar quality for $^{6}\mathrm{He} \to {}^{6}\mathrm{Be}$, even though these nuclei are only semi-magic. The case of $^{10}\mathrm{He} \to {}^{10}\mathrm{Be}$ is slightly more challenging, with a doubly closed-shell initial nucleus and a partially closed-shell final nucleus. Comparing our results for $^{6}\mathrm{He} \to {}^{6}\mathrm{Be}$ with other works is complicated by the lack of renormalization-group invariance. However, Cirigliano *et al.* [16] and Pastore *et al.* [83] found absolute values that are similar to ours using a harder interaction, and Basili *et al.* [84] also agrees with our results (apart from an arbitrary sign), although they did not include three-nucleon forces.

The cases of $^{8}\mathrm{He} \to {}^{8}\mathrm{Be}$ and $^{22}\mathrm{O} \to {}^{22}\mathrm{Ne}$ are more challenging still, because the final nuclei are truly open-shell systems. Adding triples correlations to the spherical results induces a ~50% change in the first case and worsens the agreement with NCSM in the second, suggesting the need for more particle-hole excitations. Once again, however, using the deformed final state as the reference leads to results that are both consistent with the NCSM and converged at the CCSDT-1 level. Thus, the coupled-cluster results are more accurate when the open-shell (or deformed) nucleus is taken as the reference, and they agree within smaller model-space uncertainties with the NCSM benchmarks.

The benchmark calculations suggest that the two approaches (with a spherical $^{48}\mathrm{Ca}$ or a deformed $^{48}\mathrm{Ti}$ as the reference state) allow us to bracket the NME. The result from the first approach exceeds the exact NME because the imposition of spherical symmetry increases the overlap of the initial and final wave functions. The second result underestimates the exact NME, probably because the deformations of the initial and final states are quite different. Generator-coordinate methods [85] might have an advantage here, and we expect that symmetry projection would make the results more accurate.

Unfortunately, we are not able to extend the benchmarks to heavier nuclei. Benchmarks with the traditional shell model are complicated because coupled-cluster theory in its singles, doubles, and triples approximation does not accurately capture the strong correlations in small shell-model spaces [86]; see Supplemental Material [60] for more details.

Although the coupling strength of the leading-order contact potential in the $0\nu\beta\beta$ operator is unknown [14–16], we attempt to estimate its effect by applying the coupled-cluster methods discussed above with the addition of a contact term, $V_c(\mathbf{r_{12}}) = 2\pi^2 g\delta(\mathbf{r}_{12})\tau_-^{(1)}\tau_-^{(2)}$, to the operator, $\hat{O}_{0\nu}$. Using a coupling strength of $g = \pm 1\ \mathrm{fm}^2$ results in a NME of $0.15 \le M^{0\nu} \le 1.02$ (see Supplemental Material [60] for details).

Two-neutrino double-β decay of ^{48}Ca.—The $2\nu\beta\beta$ decay of $^{48}\mathrm{Ca}$ was accurately predicted by Caurier *et al.* [87] before its observation [88–90]. Subsequent authors studied this decay further [91–93], and evaluations can be found in Refs. [17,94]. We compute the matrix element for the $2\nu\beta\beta$ decay of $^{48}\mathrm{Ca}$ with the 1.8/2.0 (EM) interaction and the Lanczos continued fraction method. We employ a spherical $^{48}\mathrm{Ca}$ natural-orbital basis and converge our results with respect to $N_{\max}$ and the number of $3p$-$3h$ configurations included in the wave functions of $^{48}\mathrm{Ca}$, $^{48}\mathrm{Ti}$, and the intermediate nucleus $^{48}\mathrm{Sc}$. The results are also converged with respect to the number of Lanczos iterations used in the continued fraction (5). We note that the $2\nu\beta\beta$ calculations can only be performed in the spherical scheme since we sum over intermediate states with definite spin.

Figure 3 shows the NME for the $2\nu\beta\beta$ decay of $^{48}\mathrm{Ca}$, computed in the CCSDT-1 approximation, as a function the energy difference, $E_I - E_F$, with different curves representing both the $N_{\max}$ convergence and $\mathcal{E}_3$ convergence of $^{48}\mathrm{Sc}$. The converged result, $M^{2\nu} = 0.065 \pm 0.002$, is at the intersection with the theoretical energy difference between the ground-state energies of $^{48}\mathrm{Ca}$ and $^{48}\mathrm{Ti}$ computed from

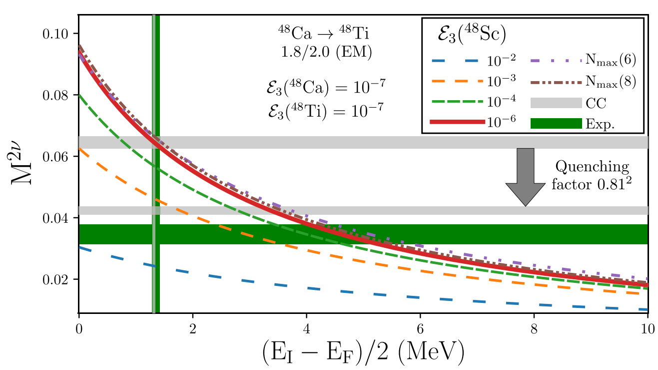

FIG. 3. The NME for the $2\nu\beta\beta$ decay $^{48}\mathrm{Ca} \to {}^{48}\mathrm{Ti}$ computed with the 1.8/2.0 (EM) interaction as a function of the energy difference, $E_I - E_F$, and the $3p-3h$ truncation used to calculate $^{48}\mathrm{Sc}$, $\mathcal{E}_3$, at $N_{\max} = 10$. The results for $N_{\max} = 6$, 8 are also shown. The experimental NME and energy difference are shown along with the computed energy difference and NME, with and without a quenching factor of 0.81^2 deduced from two-body currents [95].

the corresponding reference states, $(E_I - E_F)/2 = 1.32$ MeV. Given that E is equivalent to the negative binding energy, $E = -BE$, this is consistent with the experimental difference, $[BE(^{48}\mathrm{Ti}) - BE(^{48}\mathrm{Ca})]/2 = 1.35$ MeV. The uncertainty in our result represents the error from the different convergence criteria. These results are sensitive to the energy of the first 1^+ state in ^{48}Sc. Our value of $\Delta E_{\mu=0} = 2.93$ MeV is close to the corresponding experimental value of $BE(^{48}\mathrm{Ca}) - BE(^{48}\mathrm{Sc}^{1^+}_{\mu=0}) = 3.02$ MeV, and the NME gets reduced by about 2% if one uses the experimental datum instead. The comparison of the values in Eq. (4) to experiment are detailed in the Supplemental Material [60].

We multiply our matrix element with the quenching factor $q^2 = 0.81^2$ deduced from two-body currents in a recent coupled-cluster computation of the Ikeda sum rule in ^{48}Ca [95] which includes all final 1^+ states in ^{48}Sc and is similar to Eq. (4). We obtain $q^2 M^{2\nu} = 0.042 \pm 0.001$, which is somewhat larger than the experimental value of $M^{2\nu} = 0.035 \pm 0.003$ [94,96]. This is most likely due to our inability to accurately describe the deformed nature of ^{48}Ti. In a future work we will investigate the role of momentum dependent two-body currents on this decay. We note that the quenching factor from the Ikeda sum-rule weights all 1^+ states equally (as there is no energy denominator) and is somewhat larger than the phenomenological value of $q^2 = 0.74^2$ [97]. We verified our methods by performing two $2\nu\beta\beta$ benchmarks, of ^{48}Ca in the pf shell and of ^{14}C in a full no-core model space, which are shown in the Supplemental Material [60]. The former is compared with exact diagonalization, and the latter with the NCSM.

Conclusions.—Using interactions from chiral EFT and the coupled-cluster method, we computed the nuclear matrix elements for $0\nu\beta\beta$-decay of $^{48}\mathrm{Ca} \rightarrow {}^{48}\mathrm{Ti}$ and found a relatively small value. The uncertainties stem from the treatment of nuclear deformation and are supported by extensive benchmarks. We also calculated the $2\nu\beta\beta$-decay of $^{48}\mathrm{Ca} \rightarrow {}^{48}\mathrm{Ti}$ and included the *ab initio* quenching factor from two-body currents of the Ikeda sum rule in ^{48}Ca.

The Department of Energy will provide public access to these results of federally sponsored research in accordance with the DOE Public Access Plan [98].

We thank A. Belley, V. Cirigliano, J. de Vries, H. Hergert, J. D. Holt, M. Horoi, J. Menéndez, C. G. Payne, S. R. Stroberg, A. Walker-Loud, and J. M. Yao for useful discussions. This work was supported by the Office of Nuclear Physics, U.S. Department of Energy, under Grants No. DE-FG02-96ER40963, No. DE-FG02-97ER41019, and No. DE-SC0008499 (NUCLEI SciDAC collaboration), the Field Work Proposal ERKBP57 at Oak Ridge National Laboratory (ORNL) and SCW1579 at Lawrence Livermore National Laboratory (LLNL), the National Research Council of Canada, and NSERC, under Grants No. SAPIN-2016-00033 and No. PGSD3-535536-2019. TRIUMF receives federal funding via a contribution agreement with the National Research Council of Canada. This work was prepared in part by LLNL under Contract No. DE-AC52-07NA27344. Computer time was provided by the Innovative and Novel Computational Impact on Theory and Experiment (INCITE) program. This research used resources of the Oak Ridge Leadership Computing Facility located at ORNL. ORNL is managed by UT-Battelle, LLC under Contract No. DE-AC05-00OR22725 with the U.S. Department of Energy. The U.S. Government retains and the publisher, by accepting the article for publication, acknowledges that the U.S. Government retains a nonexclusive, paid-up, irrevocable, worldwide license to publish or reproduce the published form of this manuscript or allows others to do so for U.S. Government purposes.

[1] W. H. Furry, On transition probabilities in double beta-disintegration, Phys. Rev. **56**, 1184 (1939).

[2] J. Schechter and J. W. F. Valle, Neutrinoless double-β decay in $\mathrm{su}(2) \times u(1)$ theories, Phys. Rev. D **25**, 2951 (1982).

[3] P. Minkowski, $\mu \rightarrow e\gamma$ at a rate of one out of 109 muon decays?, Phys. Lett. **67B**, 421 (1977).

[4] R. N. Mohapatra and G. Senjanović, Neutrino Mass and Spontaneous Parity Nonconservation, Phys. Rev. Lett. **44**, 912 (1980).

[5] S. Davidson, E. Nardi, and Y. Nir, Leptogenesis, Phys. Rep. **466**, 105 (2008).

[6] G. Anton *et al.*, (EXO-200 Collaboration), Search for Neutrinoless Double-β Decay with the Complete EXO-200 Dataset, Phys. Rev. Lett. **123**, 161802 (2019).

[7] S. I. Alvis *et al.* (Majorana Collaboration), Search for neutrinoless double-β decay in ^{76}Ge with 26 kg yr of exposure from the majorana demonstrator, Phys. Rev. C **100**, 025501 (2019).

[8] M. Agostini *et al.*, Probing majorana neutrinos with double-β decay, Science **365**, 1445 (2019).

[9] J. Engel and J. Menéndez, Status and future of nuclear matrix elements for neutrinoless double-beta decay: A review, Rep. Prog. Phys. **80**, 046301 (2017).

[10] U. van Kolck, Few-nucleon forces from chiral Lagrangians, Phys. Rev. C **49**, 2932 (1994).

[11] P. F. Bedaque and U. van Kolck, Effective field theory for few-nucleon systems, Annu. Rev. Nucl. Part. Sci. **52**, 339 (2002).

[12] E. Epelbaum, H.-W. Hammer, and U.-G. Meißner, Modern theory of nuclear forces, Rev. Mod. Phys. **81**, 1773 (2009).

[13] R. Machleidt and D. R. Entem, Chiral effective field theory and nuclear forces, Phys. Rep. **503**, 1 (2011).

[14] V. Cirigliano, W. Dekens, J. de Vries, M. L. Graesser, E. Mereghetti, S. Pastore, and U. van Kolck, New Leading Contribution to Neutrinoless Double-β Decay, Phys. Rev. Lett. **120**, 202001 (2018).

[15] V. Cirigliano, W. Detmold, A. Nicholson, and P. Shanahan, Lattice QCD inputs for nuclear double beta decay, Prog. Part. Nucl. Phys. **112**, 103771 (2020).

[16] V. Cirigliano, W. Dekens, J. de Vries, M. L. Graesser, E. Mereghetti, S. Pastore, M. Piarulli, U. van Kolck, and R. B. Wiringa, Renormalized approach to neutrinoless double-β decay, Phys. Rev. C **100**, 055504 (2019).
[17] A. S. Barabash, Average and recommended half-life values for two-neutrino double beta decay, Nucl. Phys. **A935**, 52 (2015).
[18] G. Hagen, A. Ekström, C. Forssén, G. R. Jansen, W. Nazarewicz, T. Papenbrock, K. A. Wendt, S. Bacca, N. Barnea, B. Carlsson, C. Drischler, K. Hebeler, M. Hjorth-Jensen, M. Miorelli, G. Orlandini, A. Schwenk, and J. Simonis, Neutron and weak-charge distributions of the ^{48}Ca nucleus, Nat. Phys. **12**, 186 (2016).
[19] K. Tetsuno *et al.*, Status of ^{48}Ca double beta decay search and its future prospect in CANDLES, J. Phys. Conf. Ser. **1468**, 012132 (2020).
[20] J. M. Yao, B. Bally, J. Engel, R. Wirth, T. R. Rodríguez, and H. Hergert, *Ab Initio* Treatment of Collective Correlations and the Neutrinoless Double Beta Decay of ^{48}Ca, Phys. Rev. Lett. **124**, 232501 (2020).
[21] L. Coraggio, A. Gargano, N. Itaco, R. Mancino, and F. Nowacki, Calculation of the neutrinoless double-β decay matrix element within the realistic shell model, Phys. Rev. C **101**, 044315 (2020).
[22] F. Šimkovic, V. Rodin, A. Faessler, and P. Vogel, $0\nu\beta\beta$ and $2\nu\beta\beta$ nuclear matrix elements, quasiparticle random-phase approximation, and isospin symmetry restoration, Phys. Rev. C **87**, 045501 (2013).
[23] J. Barea, J. Kotila, and F. Iachello, $0\nu\beta\beta$ and $2\nu\beta\beta$ nuclear matrix elements in the interacting boson model with isospin restoration, Phys. Rev. C **91**, 034304 (2015).
[24] N. L. Vaquero, T. R. Rodríguez, and J. L. Egido, Shape and Pairing Fluctuation Effects on Neutrinoless Double Beta Decay Nuclear Matrix Elements, Phys. Rev. Lett. **111**, 142501 (2013).
[25] J. M. Yao, L. S. Song, K. Hagino, P. Ring, and J. Meng, Systematic study of nuclear matrix elements in neutrinoless double-β decay with a beyond-mean-field covariant density functional theory, Phys. Rev. C **91**, 024316 (2015).
[26] R. A. Sen'kov and M. Horoi, Neutrinoless double-β decay of ^{48}Ca in the shell model: Closure versus nonclosure approximation, Phys. Rev. C **88**, 064312 (2013).
[27] J. Menéndez, A. Poves, E. Caurier, and F. Nowacki, Disassembling the nuclear matrix elements of the neutrinoless $\beta\beta$ decay, Nucl. Phys. **A818**, 139 (2009).
[28] A. A. Kwiatkowski, T. Brunner, J. D. Holt, A. Chaudhuri, U. Chowdhury, M. Eibach, J. Engel, A. T. Gallant, A. Grossheim, M. Horoi, A. Lennarz, T. D. Macdonald, M. R. Pearson, B. E. Schultz, M. C. Simon, R. A. Senkov, V. V. Simon, K. Zuber, and J. Dilling, New determination of double-β-decay properties in ^{48}Ca: High-precision $Q_{\beta\beta}$-value measurement and improved nuclear matrix element calculations, Phys. Rev. C **89**, 045502 (2014).
[29] Y. Iwata, N. Shimizu, T. Otsuka, Y. Utsuno, J. Menéndez, M. Honma, and T. Abe, Large-Scale Shell-Model Analysis of the Neutrinoless $\beta\beta$ Decay of ^{48}Ca, Phys. Rev. Lett. **116**, 112502 (2016).
[30] A. Belley, C. G. Payne, S. R. Stroberg, T. Miyagi, and J. D. Holt, *Ab Initio* Neutrinoless Double-Beta Decay Matrix Elements for ^{48}Ca, ^{76}Ge, and ^{82}Se, Phys. Rev. Lett. **126**, 042502 (2021).
[31] K. Hebeler, S. K. Bogner, R. J. Furnstahl, A. Nogga, and A. Schwenk, Improved nuclear matter calculations from chiral low-momentum interactions, Phys. Rev. C **83**, 031301(R) (2011).
[32] A. Tichai, J. Müller, K. Vobig, and R. Roth, Natural orbitals for *ab initio* no-core shell model calculations, Phys. Rev. C **99**, 034321 (2019).
[33] S. J. Novario, G. Hagen, G. R. Jansen, and T. Papenbrock, Charge radii of exotic neon and magnesium isotopes, Phys. Rev. C **102**, 051303 (2020).
[34] G. Hagen, T. Papenbrock, D. J. Dean, A. Schwenk, A. Nogga, M. Włoch, and P. Piecuch, Coupled-cluster theory for three-body Hamiltonians, Phys. Rev. C **76**, 034302 (2007).
[35] R. Roth, S. Binder, K. Vobig, A. Calci, J. Langhammer, and P. Navrátil, Medium-Mass Nuclei with Normal-Ordered Chiral $NN + 3N$ Interactions, Phys. Rev. Lett. **109**, 052501 (2012).
[36] F. Coester, Bound states of a many-particle system, Nucl. Phys. **7**, 421 (1958).
[37] F. Coester and H. Kümmel, Short-range correlations in nuclear wave functions, Nucl. Phys. **17**, 477 (1960).
[38] J. Čížek, On the correlation problem in atomic and molecular systems. Calculation of wavefunction components in Ursell-type expansion using quantum-field theoretical methods, J. Chem. Phys. **45**, 4256 (1966).
[39] J. Čížek, On the use of the cluster expansion and the technique of diagrams in calculations of correlation effects in atoms and molecules, in *Advances in Chemical Physics* (John Wiley & Sons, Inc., New York, 2007), pp. 35–89.
[40] H. Kümmel, K. H. Lührmann, and J. G. Zabolitzky, Many-fermion theory in expS- (or coupled cluster) form, Phys. Rep. **36**, 1 (1978).
[41] R. J. Bartlett and M. Musiał, Coupled-cluster theory in quantum chemistry, Rev. Mod. Phys. **79**, 291 (2007).
[42] G. Hagen, T. Papenbrock, M. Hjorth-Jensen, and D. J. Dean, Coupled-cluster computations of atomic nuclei, Rep. Prog. Phys. **77**, 096302 (2014).
[43] J. D. Watts, J. Gauss, and R. J. Bartlett, Coupled-cluster methods with noniterative triple excitations for restricted open-shell Hartree-Fock and other general single determinant reference functions. Energies and analytical gradients, J. Chem. Phys. **98**, 8718 (1993).
[44] J. D. Watts and R. J. Bartlett, Economical triple excitation equation-of-motion coupled-cluster methods for excitation energies, Chem. Phys. Lett. **233**, 81 (1995).
[45] I. Shavitt and R. J. Bartlett, *Many-Body Methods in Chemistry and Physics* (Cambridge University Press, Cambridge, England, 2009).
[46] G. R. Jansen, M. Hjorth-Jensen, G. Hagen, and T. Papenbrock, Toward open-shell nuclei with coupled-cluster theory, Phys. Rev. C **83**, 054306 (2011).
[47] G. R. Jansen, Spherical coupled-cluster theory for open-shell nuclei, Phys. Rev. C **88**, 024305 (2013).
[48] G. Hagen, M. Hjorth-Jensen, G. R. Jansen, R. Machleidt, and T. Papenbrock, Continuum Effects and Three-Nucleon Forces in Neutron-Rich Oxygen Isotopes, Phys. Rev. Lett. **108**, 242501 (2012).

[49] G. Hagen, M. Hjorth-Jensen, G. R. Jansen, R. Machleidt, and T. Papenbrock, Evolution of Shell Structure in Neutron-Rich Calcium Isotopes, Phys. Rev. Lett. **109**, 032502 (2012).

[50] S. Binder, J. Langhammer, A. Calci, P. Navrátil, and R. Roth, Ab initio calculations of medium-mass nuclei with explicit chiral $3N$ interactions, Phys. Rev. C **87**, 021303(R) (2013).

[51] C. G. Payne, S. Bacca, G. Hagen, W. G. Jiang, and T. Papenbrock, Coherent elastic neutrino-nucleus scattering on ^{40}Ar from first principles, Phys. Rev. C **100**, 061304(R) (2019).

[52] H. N. Liu *et al.*, How Robust is the $N = 34$ Subshell Closure? First Spectroscopy of ^{52}Ar, Phys. Rev. Lett. **122**, 072502 (2019).

[53] P. Ring and P. Schuck, *The Nuclear Many-Body Problem* (Springer, Heidelberg, 1980).

[54] T. Duguet, Symmetry broken and restored coupled-cluster theory: I. Rotational symmetry and angular momentum, J. Phys. G **42**, 025107 (2015).

[55] T. M. Henderson, J. Zhao, G. E. Scuseria, Y. Qiu, T. M. Henderson, and G. E. Scuseria, Projected coupled cluster theory, J. Chem. Phys. **147**, 064111 (2017).

[56] T. Tsuchimochi and S. L. Ten-no, Orbital-invariant spin-extended approximate coupled-cluster for multi-reference systems, J. Chem. Phys. **149**, 044109 (2018).

[57] V. Cirigliano, W. Dekens, E. Mereghetti, and A. Walker-Loud, Neutrinoless double-β decay in effective field theory: The light-majorana neutrino-exchange mechanism, Phys. Rev. C **97**, 065501 (2018).

[58] F. Šimkovic, A. Faessler, V. Rodin, P. Vogel, and J. Engel, Anatomy of the $0\nu\beta\beta$ nuclear matrix elements, Phys. Rev. C **77**, 045503 (2008).

[59] Here τ^- changes a neutron into a proton.

[60] See Supplemental Material at http://link.aps.org/supplemental/10.1103/PhysRevLett.126.182502 for calculations involved in the $0\nu\beta\beta$ and $2\nu\beta\beta$ decays of ^{48}Ca and several benchmark nuclei, which includes Refs. [61–72].

[61] J. Menéndez, T. R. Rodríguez, G. Martínez-Pinedo, and A. Poves, Correlations and neutrinoless $\beta\beta$ decay nuclear matrix elements of pf-shell nuclei, Phys. Rev. C **90**, 024311 (2014).

[62] M. Honma, T. Otsuka, B. A. Brown, and T. Mizusaki, New effective interaction for pf-shell nuclei and its implications for the stability of the $N = Z = 28$ closed core, Phys. Rev. C **69**, 034335 (2004).

[63] A. Poves, J. Sánchez-Solano, E. Caurier, and F. Nowacki, Shell model study of the isobaric chains $A = 50$, $A = 51$ and $A = 52$, Nucl. Phys. **A694**, 157 (2001).

[64] M. Urban, J. Noga, S. J. Cole, and R. J. Bartlett, Towards a full ccsdt model for electron correlation, J. Chem. Phys. **83**, 4041 (1985).

[65] J. Noga, R. J. Bartlett, and M. Urban, Towards a full CCSDT model for electron correlation. CCSDT-n models, Chem. Phys. Lett. **134**, 126 (1987).

[66] C. F. Jiao, M. Horoi, and A. Neacsu, Neutrinoless double-β decay of ^{124}Sn, ^{130}Te, and ^{136}Xe in the hamiltonian-based generator-coordinate method, Phys. Rev. C **98**, 064324 (2018).

[67] J. C. Light, I. P. Hamilton, and J. V. Lill, Generalized discrete variable approximation in quantum mechanics, J. Chem. Phys. **82**, 1400 (1985).

[68] D. Baye and P.-H. Heenen, Generalised meshes for quantum mechanical problems, J. Phys. A **19**, 2041 (1986).

[69] J. C. Light and T. Carrington, Discrete-variable representations and their utilization, in *Advances in Chemical Physics* (John Wiley & Sons, Inc., New York, 2007), pp. 263–310.

[70] R. G. Littlejohn, M. Cargo, T. Carrington, K. A. Mitchell, and B. Poirier, A general framework for discrete variable representation basis sets, J. Chem. Phys. **116**, 8691 (2002).

[71] A. Bulgac and M. McNeil Forbes, Use of the discrete variable representation basis in nuclear physics, Phys. Rev. C **87**, 051301(R) (2013).

[72] S. Binder, A. Ekström, G. Hagen, T. Papenbrock, and K. A. Wendt, Effective field theory in the harmonic oscillator basis, Phys. Rev. C **93**, 044332 (2016).

[73] P. Vogel, Nuclear structure and double beta decay, J. Phys. G **39**, 124002 (2012).

[74] J. Kotila and F. Iachello, Phase-space factors for double-β decay, Phys. Rev. C **85**, 034316 (2012).

[75] J. Engel, W. C. Haxton, and P. Vogel, Effective summation over intermediate states in double-beta decay, Phys. Rev. C **46**, R2153 (1992).

[76] W. C. Haxton, K. M. Nollett, and K. M. Zurek, Piecewise moments method: Generalized lanczos technique for nuclear response surfaces, Phys. Rev. C **72**, 065501 (2005).

[77] M. A. Marchisio, N. Barnea, W. Leidemann, and G. Orlandini, Efficient method for lorentz integral transforms of reaction cross sections, Few-Body Syst. **33**, 259 (2003).

[78] M. Miorelli, S. Bacca, N. Barnea, G. Hagen, G. R. Jansen, G. Orlandini, and T. Papenbrock, Electric dipole polarizability from first principles calculations, Phys. Rev. C **94**, 034317 (2016).

[79] J. Rotureau, P. Danielewicz, G. Hagen, F. M. Nunes, and T. Papenbrock, Optical potential from first principles, Phys. Rev. C **95**, 024315 (2017).

[80] P. Navrátil, J. P. Vary, and B. R. Barrett, Large-basis *ab initio* no-core shell model and its application to ^{12}**C**, Phys. Rev. C **62**, 054311 (2000).

[81] P. Navrátil, S. Quaglioni, I. Stetcu, and B. R. Barrett, Recent developments in no-core shell-model calculations, J. Phys. G **36**, 083101 (2009).

[82] B. R. Barrett, P. Navrátil, and J. P. Vary, Ab initio no core shell model, Prog. Part. Nucl. Phys. **69**, 131 (2013).

[83] S. Pastore, J. Carlson, V. Cirigliano, W. Dekens, E. Mereghetti, and R. B. Wiringa, Neutrinoless double-β decay matrix elements in light nuclei, Phys. Rev. C **97**, 014606 (2018).

[84] R. A. M. Basili, J. M. Yao, J. Engel, H. Hergert, M. Lockner, P. Maris, and J. P. Vary, Benchmark neutrinoless double-β decay matrix elements in a light nucleus, Phys. Rev. C **102**, 014302 (2020).

[85] T. R. Rodríguez and G. Martinez-Pinedo, Neutrinoless double beta decay studied with configuration mixing methods, Prog. Part. Nucl. Phys. **66**, 436 (2011).

[86] M. Horoi, J. R. Gour, M. Włoch, M. D. Lodriguito, B. A. Brown, and P. Piecuch, Coupled-Cluster and Configuration-Interaction Calculations for Heavy Nuclei, Phys. Rev. Lett. **98**, 112501 (2007).

[87] E. Caurier, A. Poves, and A. P. Zuker, A full $0\hbar\omega$ description of the $2\nu\beta\beta$ decay of ^{48}Ca, Phys. Lett. B **252**, 13 (1990).

[88] A. Balysh, A. De Silva, V. I. Lebedev, K. Lou, M. K. Moe, M. A. Nelson, A. Piepke, A. Pronskiy, M. A. Vient, and P. Vogel, Double Beta Decay of ^{48}Ca, Phys. Rev. Lett. **77**, 5186 (1996).

[89] V. B. Brudanin, N. I. Rukhadze, Ch. Briancon, V. G. Egorov, V. E. Kovalenko, A. Kovalik, A. V. Salamatin, I. Štekl, V. V. Tsoupko-Sitnikov, Ts. Vylov, and P. Čermák, Search for double beta decay of ^{48}Ca in the TGV experiment, Phys. Lett. B **495**, 63 (2000).

[90] R. Arnold *et al.* (NEMO-3 Collaboration), Measurement of the double-beta decay half-life and search for the neutrinoless double-beta decay of ^{48}Ca with the NEMO-3 detector, Phys. Rev. D **93**, 112008 (2016).

[91] M. Horoi, S. Stoica, and B. A. Brown, Shell-model calculations of two-neutrino double-β decay rates of ^{48}Ca with the GXPF1A interaction, Phys. Rev. C **75**, 034303 (2007).

[92] C. M. Raduta, A. A. Raduta, and I. I. Ursu, New theoretical results for $2\nu\beta\beta$ decay within a fully renormalized proton-neutron random-phase approximation approach with the gauge symmetry restored, Phys. Rev. C **84**, 064322 (2011).

[93] M. Horoi, Shell model analysis of competing contributions to the double-β decay of ^{48}Ca, Phys. Rev. C **87**, 014320 (2013).

[94] A. S. Barabash, Average and recommended half-life values for two-neutrino double beta decay: Upgrade-2019, AIP Conf. Proc. **2165**, 020002 (2019).

[95] P. Gysbers, G. Hagen, J. D. Holt, G. R. Jansen, T. D. Morris, P. Navrátil, T. Papenbrock, S. Quaglioni, A. Schwenk, S. R. Stroberg, and K. A. Wendt, Discrepancy between experimental and theoretical beta-decay rates resolved from first principles, Nat. Phys. **15**, 428 (2019).

[96] S. Stoica and M. Mirea, New calculations for phase space factors involved in double-β decay, Phys. Rev. C **88**, 037303 (2013).

[97] G. Martínez-Pinedo, A. Poves, E. Caurier, and A. P. Zuker, Effective g_A in the pf shell, Phys. Rev. C **53**, R2602 (1996).

[98] http://energy.gov/downloads/doe-public-access-plan.